RSC Advances

ROYAL SOCIETY OF CHEMISTRY

www.rsc.org/advances

RSC Advances

ARTICLE

The carbon quantum dots/nickel oxide (CQDs/NiO) nanorods with high capacitance for supercapacitor

Received 00th January 20xx,
Accepted 00th January 20xx

DOI: 10.1039/x0xx00000x

www.rsc.org/

J. Xu,[a] Y. Xue,[a] J. Cao,[a*] G. Wang,[a] Y. Li,[a] W. Wang[a] and Z. Chen[a, b*]

Novel one-dimensional composites of carbon quantum dots (CQDs) coated NiO nanorods have been prepared via a facile complexation method followed by a thermal treatment process with no addition of organic solvent or surfactant. The carbon quantum dots/NiO (CQDs/NiO) nanorods are very uniform in size with an average length of about 800 nm and diameter of 30 nm. The CQDs/NiO hybrid nanorods deliver a high specific capacitance (1858 F g^{-1} at 1 A g^{-1}), exceptional rate capability (84.6%, 75.7%, 65.3%, 56.1% and 51.5% capacity retention rate at 2, 3, 5, 7 and 10 A g^{-1}, respectively) and excellent cycling stability (93% of the initial capacity retention over 1000 cycles at 2 A g^{-1}) due to the coupled effect of faradaic pseudocapacitance from the NiO nanorods and the excellent electrical conductivity of the CQDs. These outstanding electrochemical performances demonstrate that the CQDs/NiO nanorods are efficient electrode materials and have a greatly promising application in the development of high-performance electrochemical energy storage devices.

1. Introduction

Supercapacitors have occupied a very important position in clean and renewable energy field and were distinguished into electrochemical pseudocapacitors (EPCs) and double-layer capacitors (EDLCs).[1] EPCs show higher specific capacitance and energy density than EDLCs because their energy was stored through the faradic redox reactions of electro-active materials rather than the ion re-arrangement at the interface of electrode and electrolyte.[2]

Metal oxides (eg. RuO_2, NiO, MnO_2 and Co_3O_4) are extensively used as electro-active materials for EPCs. Among these investigated metal oxides, NiO was widely confirmed as an ideal electrode material due to the low cost and high environmental friendly nature. Particularly, recent research results have proved that one-dimensional (1D) NiO with special microstructure (such as nanotubes, nanowires, nanorods, and nanobelts) possessed excellent electrochemical capacitive behaviors because the electrochemical capacitance of NiO mainly comes from redox reaction on its surface and the unique 1D morphology helps to acquire a large surface area and superior electron transport.[3, 4] Using a facile and efficient soaking method, nanoporous NiO nanowires with a controllable length were prepared and demonstrated a specific capacitance of 180 F g^{-1}.[5] NiO nanotubes with a BET surface area of 239 m^2 g^{-1} were prepared by chemically depositing nickel hydroxide in anodic aluminum oxide templates and exhibited a specific capacitance of 266 F g^{-1} at a current density of 0.1 A g^{-1} and excellent specific capacitance retention of ca. 93% after 1,000 continuous charge-discharge cycles,[6] while the specific capacitance of NiO nanotube synthesized by a precursor method is 80.49 F g^{-1} when the current densities are 50 mA g^{-1}.[7] Ren et al reported that NiO nanofibers modified by citric acid were fabricated by an electrospinning process and used as electroactive materials for supercapacitor, which showed a high capacitance of 336 F g^{-1} and excellent cyclic performance after 1000 cycles.[8] In spite of these remarkable progresses, the specific capacitance of 1D NiO is much less than its theoretical value (2584 F g^{-1}) and the cycle performances still need to be further increased, which mainly comes from their high electrical resistance, small specific surface area and slow ion diffusion rate. Thus, it is quite necessary to enhance the electrical conductivity and electrochemical utilization of the 1D NiO materials to improve the energy density and power density.

Combining highly conductive carbon materials with metal oxide was demonstrated to be a reliable strategy to increase the electrochemical utilization and specific capacitance of the 1D NiO materials; because the superior features of both carbon and 1D NiO can be fully employed. For example, Zhang et al. successfully prepared 1D hollow NiO on carbon nanofibers, which showed a high specific capacitance of 642 F g^{-1} measured at a current density of 3 A g^{-1} and the total capacitance loss is only 5.6% after 1000 cycles.[9] Paravannoor et al. reported carbon-grafted NiO nanowires prepared by hydrothermal method, and the maximum capacitance was calculated to be 1.6 F in an aprotic ionic liquid.[10] Han et al.

[a] School of Petrochemical Engineering, Jiangsu Key Laboratory of Advanced Catalytic Materials and Technology, Changzhou University, Changzhou 213164, China.
[b] Jiangsu Collaborative Innovation Center of Photovolatic Science and Engineering, Jiangsu Key Laboratory of Materials Surface Science and Technology, School of Materials Science and Engineering, Changzhou 213164, China

used a simple ZnO-template method to prepare carbon fiber paper supported NiO nanotube, and a specific capacity of ca. 440 F g^{-1} was acquired at 5 mV S^{-1}.[11]

Recently, carbon quantum dots (CQDs) were considered as new environmentally friendly carbon electrode materials because of their superior conductivity and high specific surface area,[12-15] which are conductive to improve the electrons transport, ionic motion and enlarge the contact area between electrode and electrolyte. In particular, Zhu et al found the CQDs can combine with hydrous RuO_2 nanoparticles via an impregnation method and the CQDs/RuO_2 hybrid materials exhibited a high specific capacitance of 460 F g^{-1}.[16] Furthermore, Xia et al found Fe_2O_3 quantum dots doped graphene and Ag nanoparticles decorated MnO_2 nanowires have greatly improved conductivity and excellent supercapacitive performances.[17, 18] However, the use of CQDs to modify NiO is rare. In this paper, we report the facile synthesis and excellent electrochenmical performances of 1D CQDs/NiO nanorods. The surface of NiO nanorods were coated with evenly dispersed CQDs by a facile complexation method followed by a thermal treatment process. The developed 1D CQDs/NiO nanocomposites displayed distinguished supercapacitor performances, which can be attributed to the faradaic pseudocapacitance of NiO coupled with the high electrical conductivity of the CQDs.

2. Experimental Section

2.1. Reagents and Materials

Commercial $Ni(NO_3)_2{\cdot}6H_2O$ (Sigma-Aldrich Co. Ltd, USA), C_6H_5COONa (Sigma-Aldrich Co. Ltd, USA) and KOH (Sinopharm Chemical Reagent Co. Ltd, China) were analytical purity and used as received without further purification.

2.2. Preparation of CQDs/NiO

CQDs/NiO was synthesized by a complexation reaction of Ni^{2+} and $C_6H_5COO^-$ followed by a thermal copyrolysis treatment process. Firstly, an aqueous 24 mL $Ni(NO_3)_2$ solution (0.02 mol L-1) was mixed with 36 mL C_6H_5COONa solution (0.267 mol L^{-1}) under continuous stirring at room temperature. Then, the mixture was put into an autoclave and hydrothermally treated at 95 °C for 48 h. Subsequently, the resulting green product was separated by centrifugation, washed repeatedly with distilled water, and directly dried in a vacuum oven at 80 °C for 24 h. Finally, the above green precursor was heated to 500 °C and maintained for 1 h under an argon atmosphere.

2.3. Structural characterization

The elemental analysis of the C and H was conducted with the Perkin-Elmer 2400 Series II CHNS/O Elemental Analyzer. The Ni content was measured by inductively coupled plasma-atomic emission spectrometry (ICP-AES). The crystalline structure of the greenish precursor and the final product were determined by powder X-ray diffraction using Cu Kα radiation (XRD, Rigaku D/max 2500 PC) over a 2θ range of 5-90o. A Netzsch TG 209F3 thermoanalyzer was used to investigate the mass loss at different temperature. The heating rate was 10 °C min-1 and typical sample quantity used was ca. 5-10 mg. The morphological analysis was carried out by field-emission scanning electron microscope (FESEM, S4800, Hitachi) with X-ray energy dispersive spectrometer (EDS) and scanning transmission electron microscope (STEM, Tecnai G2 S-Twin F20, FEI) using microgrids as substrates. Nitrogen adsorption-desorption isotherms of the CQDs/NiO were determined at 77 K using a surface area analyzer (ASAP 2010 Micromeritics) and the specific surface area was obtained using the Barrett-Joyner-Halenda (BJH) method.

2.4. Electrochemical characterization

The working electrode of CQDs/NiO nanorod was prepared according to the following steps. Typically, 85 wt.% CQDs/NiO, 10 wt.% acetylene black as a conducting agent and 5 wt.% polytetrafluorethylene (PTFE) as a binder were homogeneously mixed together to form a slurry, which was pressed into a nickel foam (1cm×1 cm) current collector under a pressure of 8 MPa and later dried at 80 °C for 12 h.

The electrochemical behavior of the CQDs/NiO electrode was characterized by cyclic voltammetry (CV), galvanostatic charge-discharge tests and electrochemical impedance spectroscopy with the help of a VersaSTAT3 electrochemical workstation (Princeton Applied Research, USA). The CV curves were conducted in a potential range between 0 and 0.6 V versus Hg/HgO at scan rates of 2-50 mV s^{-1}. The constant current charge-discharge test was carried out at different current densities within a potential range of 0 to 0.45 V, and the cycling behavior was characterized up to 500 cycles. Electrochemical impedance spectroscopy was carried out to prove the capacitive performance at open circuit potential with a frequency range of 0.01–10^5 Hz. These electrochemical measurements were carried out at room temperature in a 6 mol L^{-1} KOH solution using a three-electrode system consisting of the CQDs/NiO electrode as working electrode, a Hg/HgO electrode as reference electrode, and a platinum plate (1cm×1 cm) as counter electrode.

3. Results and discussion

3.1. Elemental analysis of the as-prepared precursor

Based on elemental analysis results of Ni, C and H (Table 1), the precursor composition can be approximatively listed as $Ni(C_6H_5COO)_{1.17}(OH)_{0.83}{\cdot}0.59H_2O$. After heat-treatment at 500 ^oC for 1 h, the C amount in the final product is ca. 4.36%.

Table 1 Element analysis results of the as-prepared samples

Sample	Ni (%)	C (%)	H (%)	O (%)
before heating	26.08	43.70	3.51	26.71
after heating	75.16	4.36	0.02	20.46

3.2. Preparation procedure of the CQDs/NiO hybrids

The preparation procedure of the CQDs/NiO hybrid is summarized in Scheme 1. Firstly, C_6H_5COONa were used to couple Ni^{2+} and provide OH^- under hydrothermal conditions. Then, the as-prepared benzoate intercalated nickel hydroxide precursor was heat-treated under 500 °C and CQDs appeared on the surface of NiO.

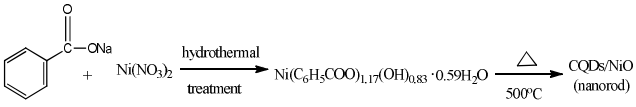

Scheme 1

3.3. Structure analysis

XRD patterns of the as-synthesized greenish precursor and final product were shown in Fig. 1. For the precursor, the diffraction peaks appeared at 5.95°, 11.85°, 14.62, 15.88 and 17.78° (Fig. 1a), corresponding to benzoate intercalated nickel hydroxide.[19-21] After been heat-treated at 500 °C, new diffraction peaks at 37.18°, 43.24°, 62.76°, 75.34° and 79.40° existed (Fig. 1b), which were indexed undisputedly to cubic NiO (JCPDS 47-1049). Additionally, these NiO diffraction peaks can be denoted as (111), (200), (220), (311) and (222) reflections, respectively. Meanwhile a broad diffraction peak centred at ca. 23.5 °C emerged (the inset in Fig. 1), which can be assigned to the diffraction pattern of the CQDs and the (220) plane of CQDs.[15] Based on the half peak width of the (220) plane of CQDs and Scherrer equation, the crystallite sizes of CQDs can be estimated to be about 4.65 nm. The above data demonstrate that the CQDs/NiO was obtained by the thermal decomposition of green precursor at 500 °C.

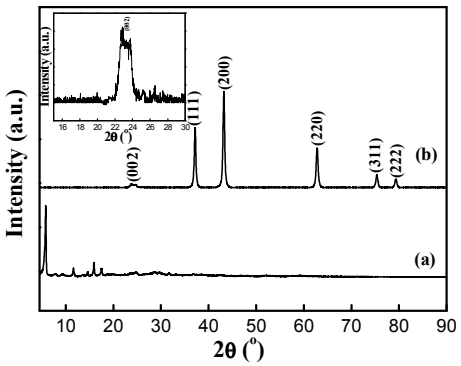

Fig. 1 XRD spectrum of the greenish precursor (a) and the final product (b). The inset shows the broad peak for CQDs.

Thermogravimetric analysis of the greenish precursor was conducted from 50 to 700 °C, as shown in Fig. 2. The weight loss is ca. 4.7 wt.%, 54.9 wt.% and 11.2 wt.% during the temperature range of 125-150 °C, 270-400 °C and 400-490 °C, which corresponds the loss of crystallization water,[22] decomposition of benzoate intercalated nickel hydroxide[23] and the formation of CQDs/NiO, respectively. Moreover, the molar ratio of crystallization water is calculated to be 0.587, which is consistent with the formula $Ni(C_6H_5COO)_{1.17}(OH)_{0.83}·0.59H_2O$.

The morphological features of the CQDs/NiO were investigated using FESEM and STEM. Fig. 3 presents the FESEM image and corresponding EDX spectrum of the CQDs/NiO. The CQDs/NiO exhibits a uniform rod-like morphology with an average length of about 800 nm and diameter of 30 nm. The NiO surface was coated with many CQDs nanoparticles, which displays a coarse morphology. The EDX spectrum of the CQDs/NiO nanorods shows the presence of Ni, C, O and additional Pt. The Pt signals arise from the Pt coating which was applied on the sample to improve the conductivity of samples. Fig. 4 displays TEM images of the CQDs/NiO with a corresponding energy-dispersive X-ray spectroscopy (EDS) elemental mapping for Ni, C, O. The diameter of CQDs/NiO nanorods is around 30 nm and the spherical CQDs with an average size of ca. 4.6 nm were uniformly coated on the surface of 1D NiO nanorods (Fig. 4A and B), which agree well with the SEM and XRD results. A high-resolution TEM image of CQDs illustrates the clear lattice fringes with a lattice spacing of 0.219 nm (Fig. 4C), which corresponds to the (100) facet of graphitic carbon (JCPDS Card File 41-1487) and previously reported carbon dots.[24-26] Furthermore, the EDS elemental mapping shows that the distributions of Ni and O are consecutive and well-matched with each other, while the C distribution is not continuous and the signal range accords with the particle size of CQDs (Fig. 4E), proving that CQDs were well dispersed on the NiO nanorods. This special morphology helps to improve the conductivity of NiO and obtain good electrochemical properties.

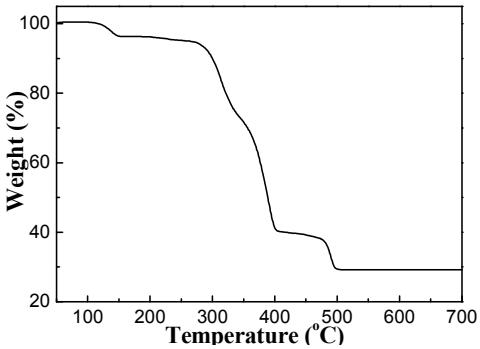

Fig. 2 Thermogravimetric analysis of the greenish precursor

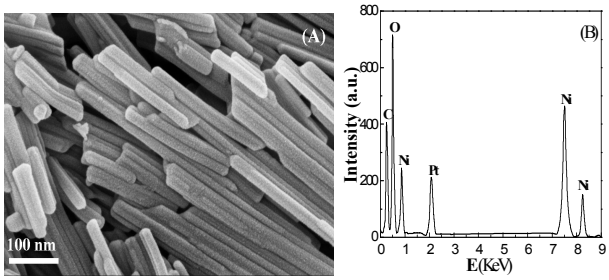

Fig. 3 FESEM images (A) with and corresponding EDX spectra (B) of the CQDs/NiO

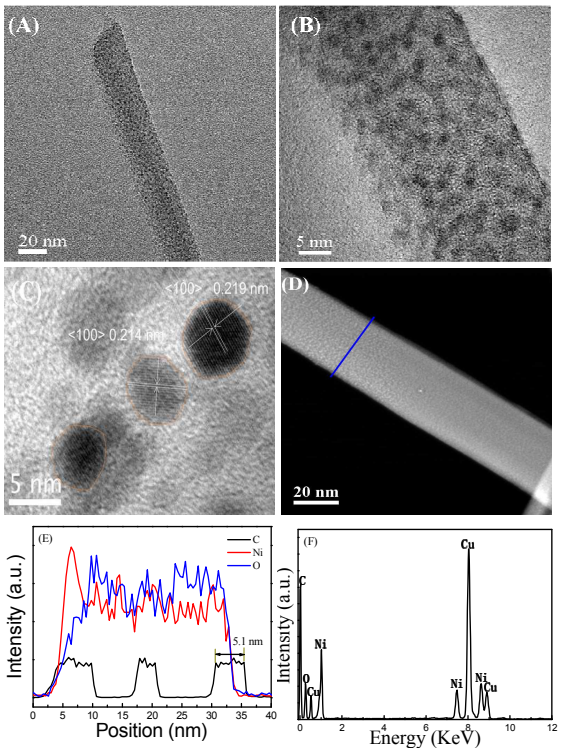

Fig. 4 TEM (A, B), HRTEM (C), STEM (D) images, element mapping (E) and STEM-EDX analysis (F) of the CQDs/NiO with different magnification.

The nitrogen adsorption-desorption isotherm and pore size distribution plots are shown in Fig. 5. For the CQDs/NiO, a hysteresis loop in the nitrogen desorption branch emerged and an obvious type IV isotherm was observed, proving the existence of abundant mesopores.[27] Furthermore, the Barrett-Joyner-Halenda (BJH) pore size distribution in the inset presented a sharp peak located at ca. 5.8 nm, which is just in the reported optimum range of 3-13 nm.[28] Moreover, the Brunauer-Emmett-Teller (BET) specific surface area of NDMG is 248.6 $m^2 g^{-1}$ and the total pore volume reaches 0.86 $cm^3 g^{-1}$.

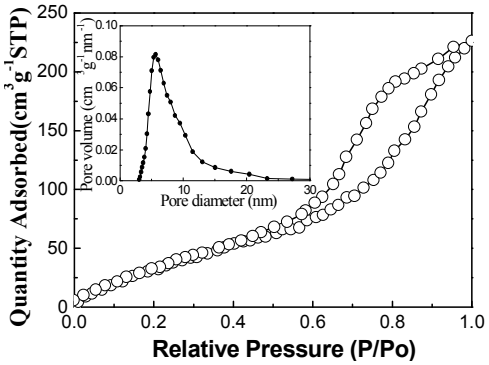

Fig. 5 Nitrogen adsorption-desorption isotherm and pore size distribution plots.

3.2. Electrochemical performances

Cyclic voltammetric (CV) curves were measured at different scan rates in a potential range of 0-0.60 V (versus Hg/HgO) to examine the electrochemical characteristics of the prepared CQDs/NiO nanorod electrodes. Fig. 6 presents the CV curves of the CQDs/NiO nanorod electrode in a three electrode system with 6 mol L^{-1} KOH as electrolyte. A pair of well-defined redox reaction peak is visible in each CV curve, indicating that the electrochemical capacitance of the CQDs/NiO nanorod electrode mainly results from the pseudocapacitance rather than the electric double-layer capacitance. Furthermore, the peak current increases with increasing scan rate from 2 to 50 mV s^{-1}, which suggests its good reversibility of fast charge-discharge response. In the present study, the electrochemical capacitance of CQDs/NiO in KOH solution is based on the redox process of NiOOH/NiO[7] and charge separation at the electrode-electrolyte interfacial layer.[29, 30] Furthermore, the redox reaction peak potential difference of the CQDs/NiO nanorods electrode is smaller than that of carbon-grafted NiO nanowires,[10] carbon fiber paper supported NiO nanotube,[9,11] core-shell C@NiO nanoparticles[31] and NiO/carbon nanotubes nanocomposite[32] at a same scan rate, which reveals that the electrochemical reversibility of the CQDs/NiO nanorod electrode is excellent.

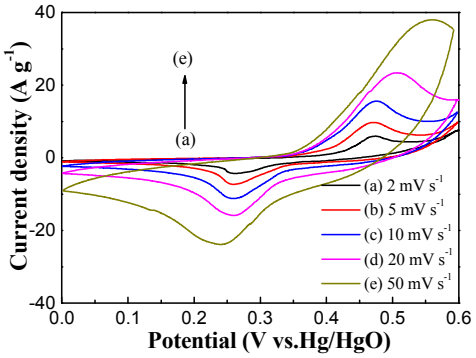

Fig. 6 CV curves of the CQDs/NiO at different scan rates.

Fig. 7 shows the galvanostatic charge-discharge behaviors of CQDs/NiO electrode in 6 mol L^{-1} KOH electrolyte within a potential range of 0-0.45 V at different current densities. As observed, the shape of the charge-discharge curve shows the characteristic of pseudocapacitance and the discharge time is approximately equal to the charge time. In addition, all of the charge-discharge curves of the CQDs/NiO electrode display two sections: a sharp potential variation (0-0.35 V) and a slow sloped alteration (0.35-0.45 V), which were separately recognized as the charge separation and the faradic redox reaction process on the electrode-electrolyte interface.[33] A very high specific capacitance of 1858 F g^{-1} is calculated from the discharge curve at 1 A g^{-1}, which is much higher than the specific capacitances of carbon fiber paper/NiO nanotube,[11] NiO/graphene,[34,35] NiO/carbon[36] and NiO/CNT.[37] Furthermore, the specific capacitance of the CQDs/NiO can attain 1572,

1406, 1214, 1042 and 956 F g^{-1} at 2, 3, 5, 7 and 10 A g^{-1}, respectively. In comparison with the specific capacitance of the CQDs/NiO nanorod at 1 A g^{-1}, the capacity retention rate is 84.6%, 75.7%, 65.3%, 56.1% and 51.5% at 2, 3, 5, 7 and 10 A g^{-1}, exhibiting an exceptional rate capability. The excellent electrochemical performances of the CQDs/NiO electrode may due to the synergic effect of CQDs and NiO, their unique 1D nanostructure and large specific surface area.

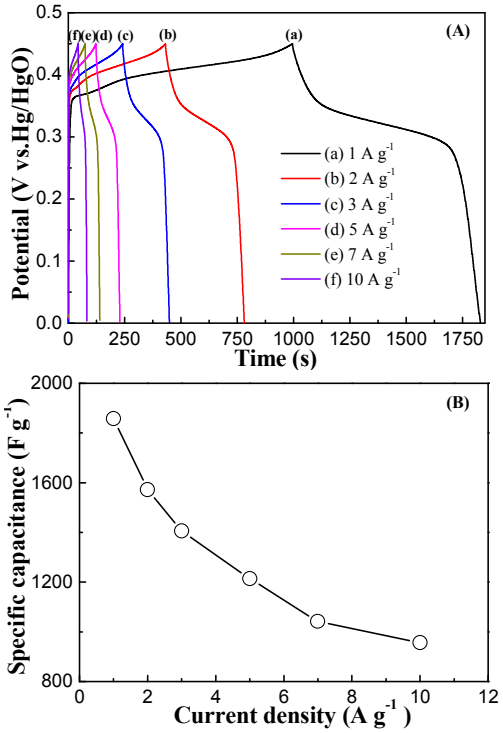

Fig. 7 Charge-discharge curves (A) and specific capacitances (B) of the CQDs/NiO electrode at different current densities.

It is critical for supercapacitor to maintain good cycling stability because it directly determines its application prospect. Galvanostatic cycling experiments were undertaken to investigate the cycle performance of the CQDs/NiO nanorod electrode. Fig. 8 shows the variation of specific capacitance of the CQDs/NiO nanorod electrode in 6 mol L^{-1} KOH electrolyte at 2 A g^{-1}. The CQDs/NiO nanorod electrode exhibited good stability and reversibility with cycling efficiency of 93% after 1000 cycles.

The typical nyquist plot of the CQDs/NiO nanorod nanocomposite was measured in a frequency range of 10^5 kHz to 0.01 Hz to determine the resistance between electrode and electrolyte, and the internal resistance of electrode, as displayed in Fig. 9. The plot shows a semicircle in the high frequency range and an inclined line in the low frequency region. From the point intersecting with the real axis in the range of high frequency, the internal resistance of the CQDs/NiO nanorod electrode in an open circuit condition is evaluated to be ca. 2.3 Ω. In the high-to medium frequency region, one narrow semicircle can be observed and the diameter is around 5.2 Ω, marking a low ion diffusion resistance and fast faradic reactions. The phase angle of the CQDs/NiO nanorod electrode in the low frequency region is higher than 45°, suggesting that the electrochemical capacitive behavior is not controlled by diffusion process. These results imply that the coating of CQDs can reduce the charge transfer resistance of the NiO and improve the electronic conduction during charge-discharge cyclic process.

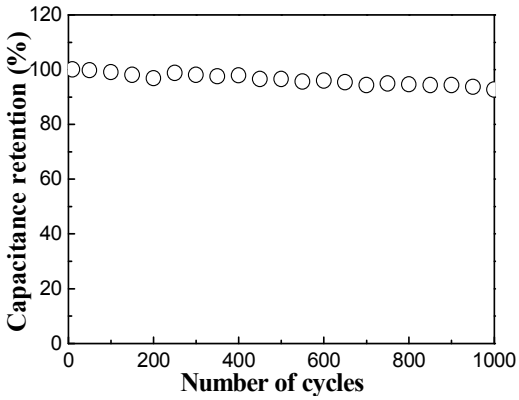

Fig.8 Cycling performance of the CQDs/NiO electrode at 2 A g^{-1}.

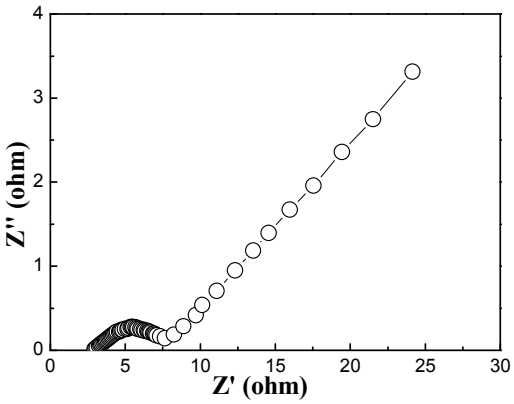

Fig. 9 Nyquist plot of the CQDs/NiO electrode.

4. Conclusions

CQDs/NiO nanorods with an average length of about 800 nm and diameter of 30 nm were synthesized and used as electroactive materials for supercapacitor. Electrochemical measurements demonstrated that the as-prepared electrode material delivered a high specific capacitance of 1858 F g^{-1} at 1 A g^{-1} and good stability over 1000 cycles. Moreover, an excellent capacitance retention rate was achieved at different charge-discharge current densities due to the unique one-dimentional structure, high electrical conductivity and large surface area of the CQDs/NiO nanorods. The distinguished electrochemical performance and facile preparation process

render the CQDs/NiO nanorods quite promising for practical application in supercapacitors.

Acknowledgements

We would like to thank the National Natural Science Foundation of China (21573025 and 51574047), the Natural Science Foundation of Jiangsu Province (12KJA150003 and BK20151183), Qing Lan Project, and the Project Funded by the Priority Academic Program Development (PAPD) of Jiangsu Higher Education Institutions for support of this work.

Notes and references

1 P. Simon and Y. Gogotsi, *Nat. Mater.*, 2008, **7**, 845-854.
2 G. Wang, L. Zhang and J. Zhang, *Chem. Soc. Rev.*, 2012, **41**, 797-828.
3 R. S. Devan, R. A. Patil, J. H. Lin and Y. R. Ma, *Adv. Funct. Mater.*, 2012, **22**, 3326-3370.
4 R. A. Patil, R. S. Devan, J. H. Lin, Y. R. Ma, P. S. Patil and Y. Liou, *Sol. Energ. Mat. Sol. C.*, 2013, **112**, 91-96.
5 H. Pang, Q. Lu, Y. Zhang, Y. Lia and F. Gao, *Nanoscale*, 2010, **2**, 920-922.
6 J. Xu, L. Gao, J. Cao, W. Wang and Z. Chen, *J. Solid State Electrochem.*, 2011, **15**, 2005-2011.
7 H. Pang, Q. Lu, Y. Lia and F. Gao, *Chem. Commun.*, 2009, **48**, 7542-7544.
8 B. Ren, M. Fan, Q. Liu, J. Wang, D. Song and X. Bai, *Electrochim. Acta*, 2013, **92**, 197-204.
9 G. Q. Zhang, L. Yu, H. E. Hoster and X. W. Lou, *Nanoscale*, 2013, **5**, 877-881.
10 A. Paravannoor, S. V. Nair, P. Pattathil, M. Mancab and A. Balakrishnan, *Chem. Commun.*, 2015, **51**, 6092-6095.
11 B. Han, E. J. Lee, J. Y. Kima, J. H. Bang, *New J. Chem.*, 2015, **39**, 1996-2003.
12 Y. Wang and A. Hu, *J. Mater. Chem. C*, 2014, **2**, 6921-6939.
13 W. W. Liu, Y. Q. Feng, X. B. Yan, J. T. Chen and Q. J. Xue, *Adv. Funct. Mater.*, 2013, **23**, 4111-4122.
14 Y. Zhu, Z. Wu, M. Jing, H. Hou, Y. Yang, Y. Zhang, X. Yang, W. Song, X. Jia, and X. Jia, *J. Mater. Chem. A*, 2015, **3**, 866-877.
15 K. Bhattacharya and P. Deb, *Dalton Trans.*, 2015, **44**, 9221-9229.
16 Y. Zhu, X. Ji, C. Pan, Q. Sun, W. Song, L. Fang, Q. Chen and C. E. Banks, *Energy Environ. Sci.*, 2013, **6**, 3665-3675.
17 H. Xia, C. Hong, B. Li, B. Zhao, Z. Lin, M. Zheng, S. V. Savilov, and S. M. Aldoshin, *Adv. Funct. Mater.,* 2015, **25**, 627-635.
18 H. Xia, C. Hong, X. Shi, B. Li, G. Yuan, Q. Yao and J. Xie, *J. Mater. Chem. A*, 2015, **3**, 1216-1221.
19 G. V. Manohara and P. V. Kamath, *Z. Anorg. Allg. Chem.*, 2014, **640**, 434-438.
20 X. Guo, L. Wang, S. Yue, D. Wang, Y. Lu, Y. Song and J. He, *Inorg. Chem.*, 2014, **53**, 12841-12847.
21 L. Poul, N. Jouini and F. Fiévet, *Chem. Mater.*, 2000, **12**, 3123-3132.
22 L. Wang, S. Lu, Y. Zhou, X. Guo, Y. Lu, J. He and D. G. Evansa, *Chem. Commun.*, 2011, **47**, 11002-11004.
23 X. Guo, L. Wang, S. Yue, D. Wang, Y. Lu, Y. Song and J. He, *Inorg. Chem.*, 2014, **53**, 12841-12847.
24 J. Hou, L. Wang, P. Zhang, Y. Xu and L. Ding, *Chem. Commun.*, 2015, **51**, 17768-17771.
25 R. K. Kokal, P. N. Kumar, M. Deepa and A. K. Srivastava, *J. Mater. Chem. A,* 2015, **3**, 20715-20726.
26 X. Chen, W. Zhang, Q. Wang and J. Fan, *Carbon*, 2014, **79**, 165-173.
27 Y. Zhu, S. Murali, M. D. Stoller, K. J. Ganesh, W. Cai, P. J. Ferreira, A. Pirkle, R. M. Wallace, K. A. Cychosz, M. Thommes, D. Su, E. A. Stach and R. S. Ruoff, *Science*, 2011, **332**, 1537-1541.
28 F. L. Braghiroli, V. Fierro, A. Szczurek, N. Stein, J. Parmentier and A. Celzard, *Ind. Crop. Prod.*, 2015, **70**, 332-340.
29 L. Hao, X. Li and L. Zhi, *Adv. Mater.*, 2013, **25**, 3899-3904.
30 M. Y. Cho, M. H. Kim, H. K. Kim, K. B. Kim, J. R. Yoon and K. C. Roh, *Electrochem. Commun.*, 2014, **47**, 5-8.
31 L. Fan, L. Tang, H. Gong, Z. Yao and R. Guo, *J. Mater. Chem.*, 2012, **22**, 16376-16381.
32 J. Y. Lee, K. Liang, K. H. An and Y. H. Lee, *Synthetic Met.*, 2005, **150**, 153-157.
33 Z. Lu, Z. Chang, J. Liu and X. Sun, *Nano Res.*, 2011, **4**, 658-665.
34 C. Wu, S. Deng, H. Wang, Y. Sun, J. Liu and H. Yan, *ACS Appl. Mater. Interfaces*, 2014, **6**, 1106-1112.
35 N. B. Trung, T. V. Tam, D. K. Dang, K. F. Babu, E. J. Kim, J. Kim and W. M. Choi, *Chem. Eng. J.*, 2015, **264**, 603-609.
36 Y. Wang, S. Xing, E. Zhang, J. Wei, H. Suo, C. Zhao and X. Zhao, *J. Mater. Sci.*, 2011, **47**, 2182-2187.
37 W. Yi, D. Yang, H. Chen, P. Liu, J. Tan and H. Li, *J. Solid State Electrochem.*, 2014, **18**, 899-908.

Graphical abstract

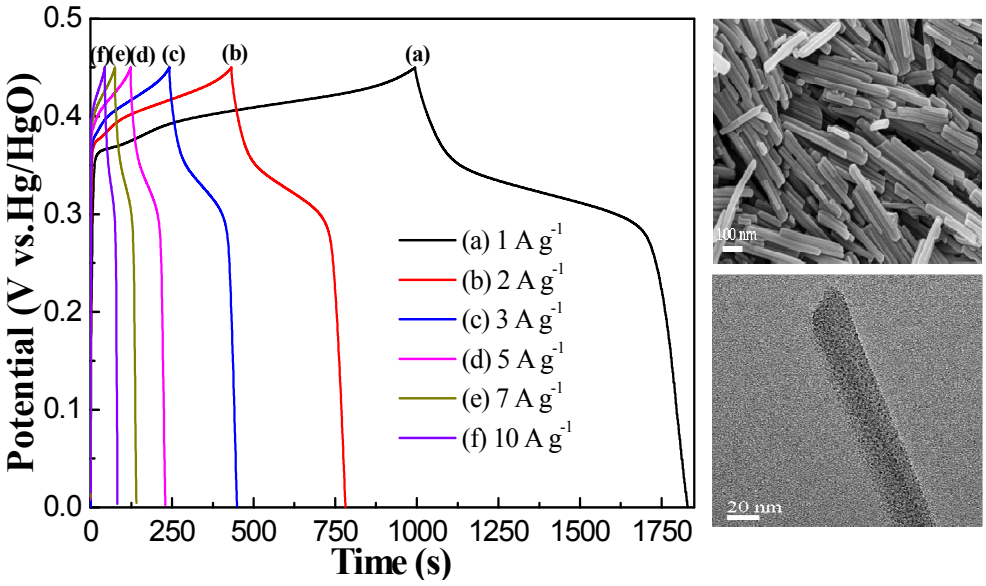

Novel one-dimensional composites of carbon quantum dots (CQDs) coated NiO nanorodes have been prepared via a facile complexation method followed by a thermal treatment process and used as electroactive materials for supercapacitor. The CQDs/NiO hybrid nanorodes deliver a high specific capacitance of 1858 F g^{-1} at 1 A g^{-1}, exceptional rate capability and excellent cycling stability.